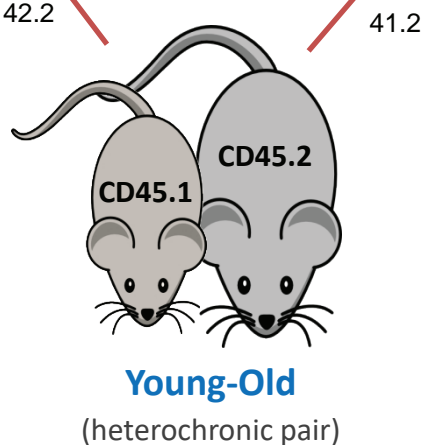
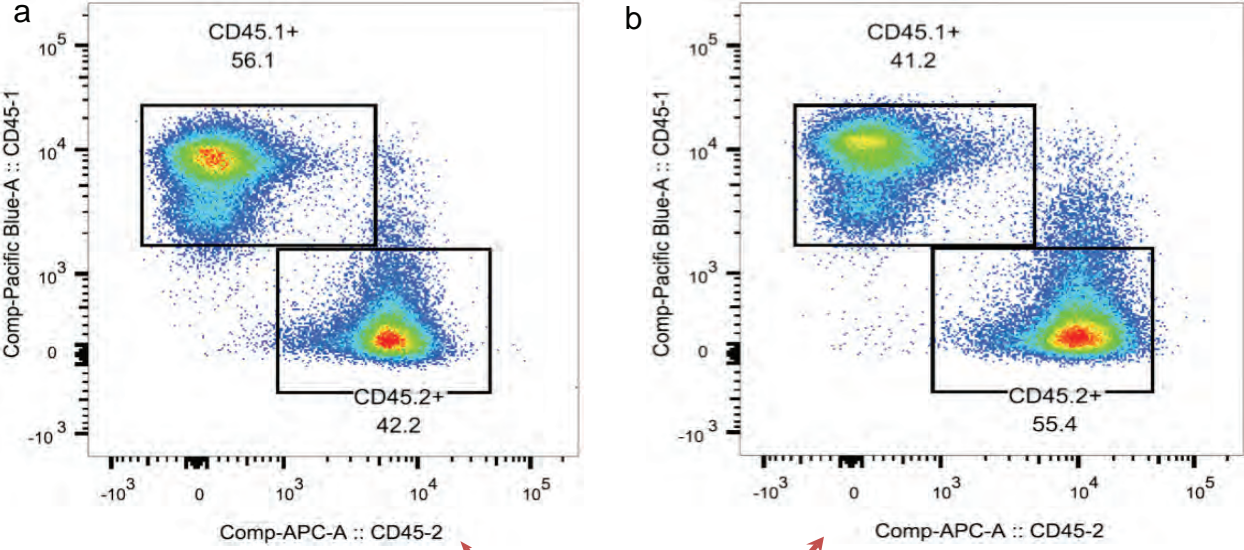


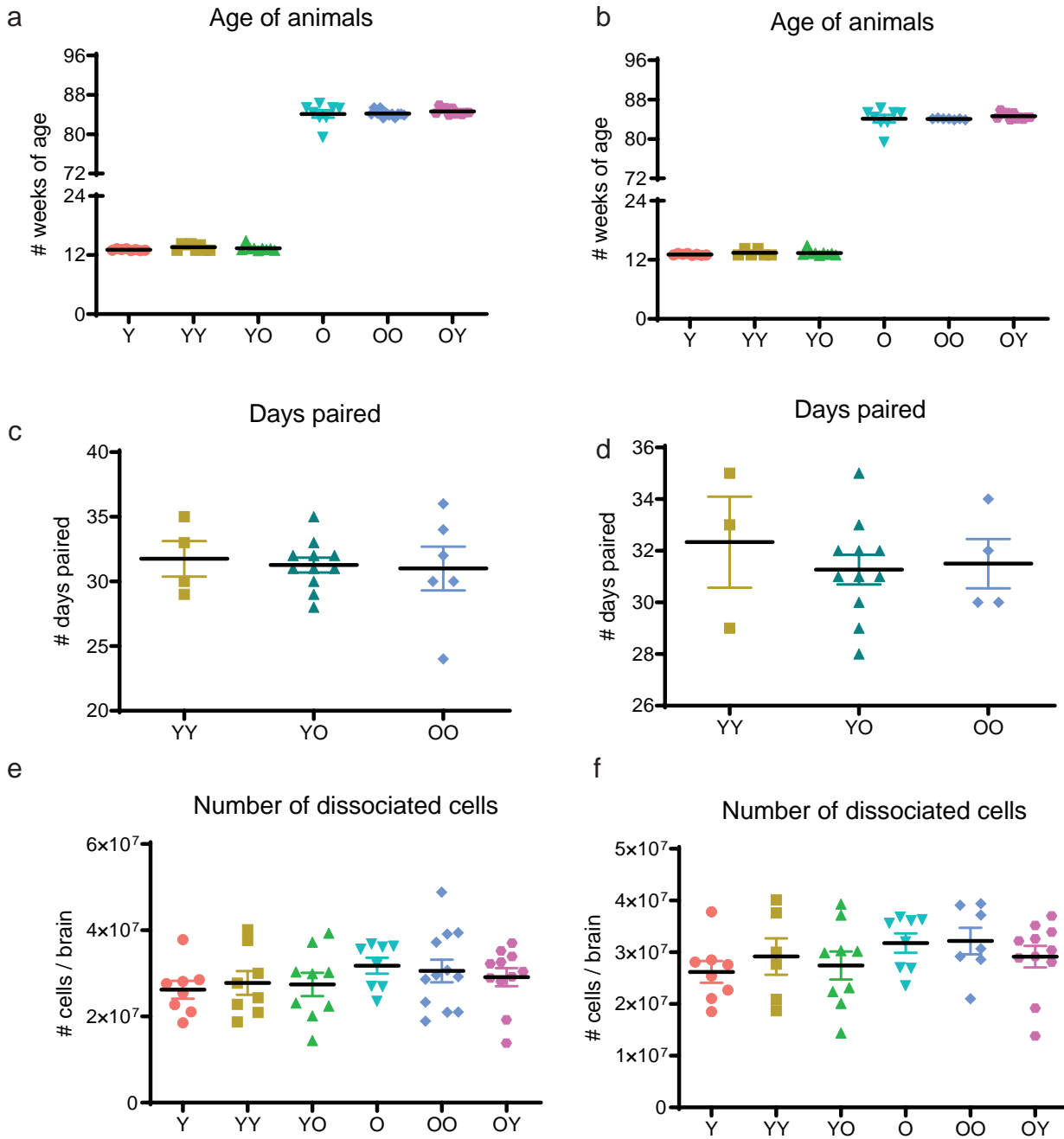
Fig_S1



Supplementary Figures

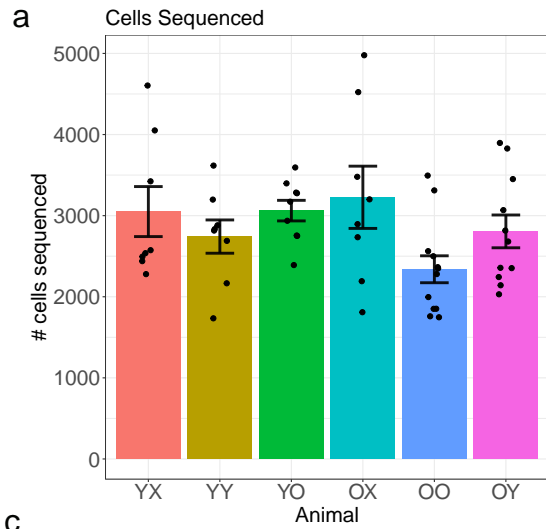
Supplementary Fig 1. Confirmation of blood chimerism. Representative flow cytometry analysis of CD45.1 and CD45.2 expression markers on splenocytes isolated from **(a)** young (CD45.1⁺) and **(b)** old mice (CD45.2⁺) following heterochronic parabiosis. In each plot, the percentage of donor-derived blood cells from one partner in the spleen of the other partner is depicted by arrows.

Fig_S2



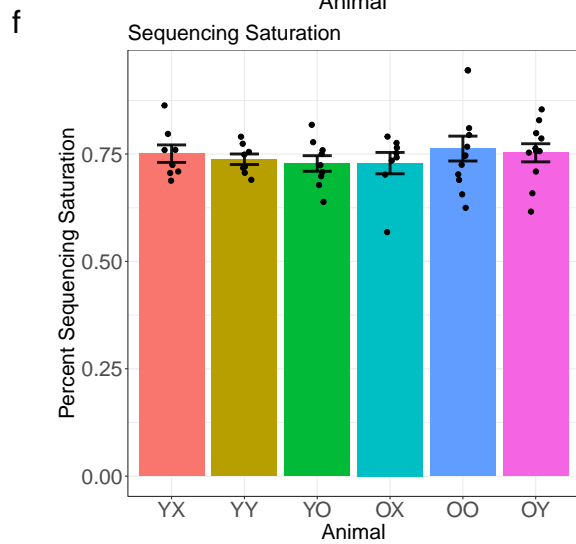
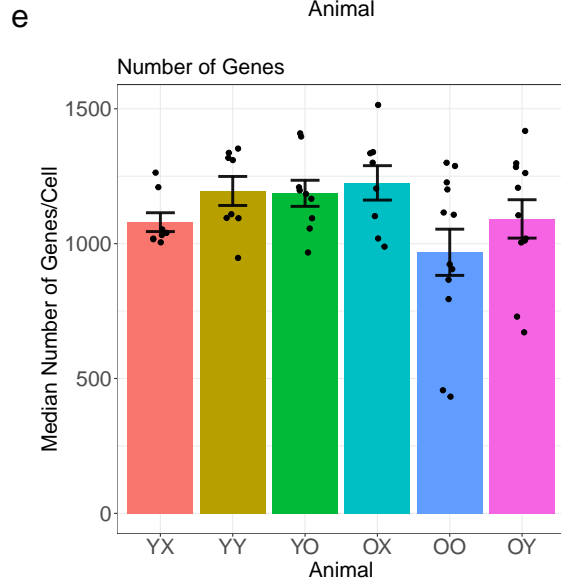
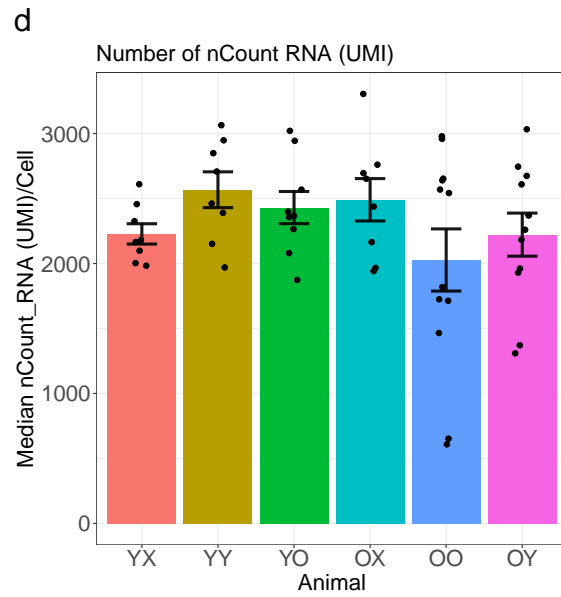
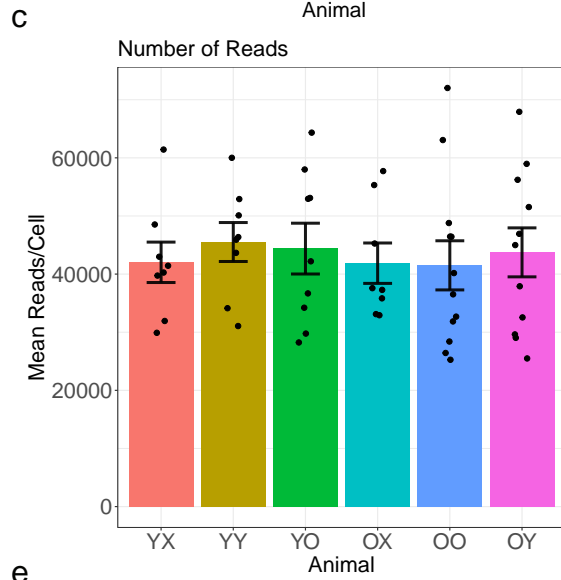
Supplementary Fig 2. Sample metrics. Profiling of animals and their derived brain cells used for sequencing, before (a,c,e) and after (b,d,f) quality control filtering in which certain animals were omitted (see Methods). **a-b.** Age of mice in weeks prior to parabiosis surgeries. **c-d.** Number of days joined across parabiotic pairs. **e-f.** Number of dissociated cells analyzed per brain across all animal types.

Fig_S3



b

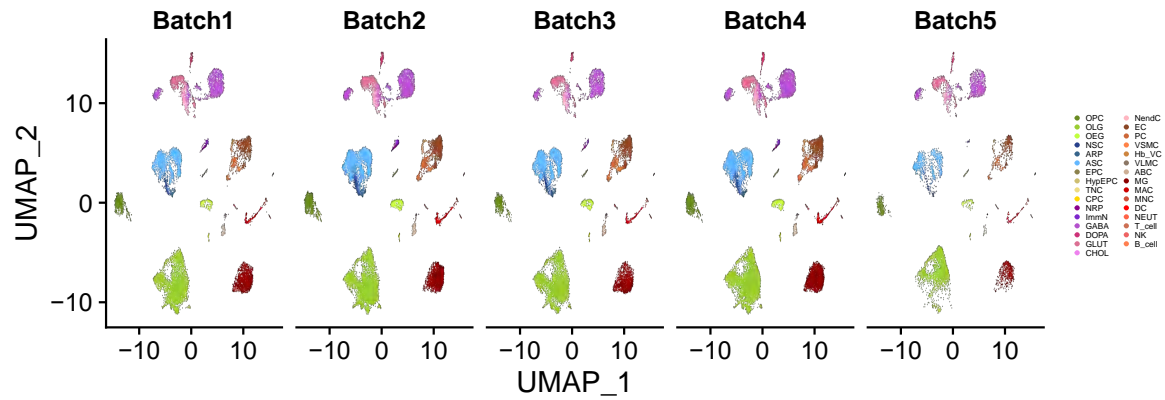
Animal	# Mice	# Cells
YX	8	24401
YY	8	21935
YO	9	27557
OX	8	25811
OO	12	28066
OY	11	30865



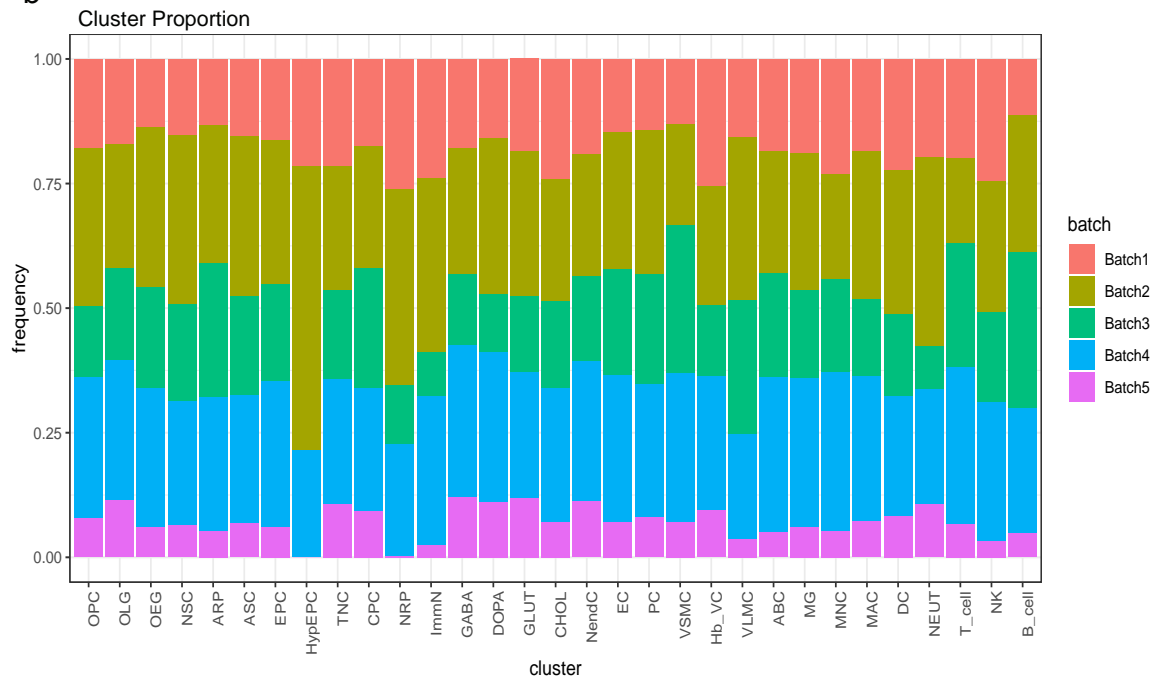
Supplementary Fig 3. Sequencing metrics. Scatter plots showing metrics of all sequenced young and old cells prior to any cell filtering: **a.** Number of cells sequenced by animal. **b.** Total number of animals and cells analyzed. **c.** Mean number of mapped reads per cell by animal. **d.** Median number of nCount RNA (UMI) detected per cell by animal. **e.** Median number of genes detected per cell by animal. Data presents mean or median \pm SEM.

Fig_S4

a

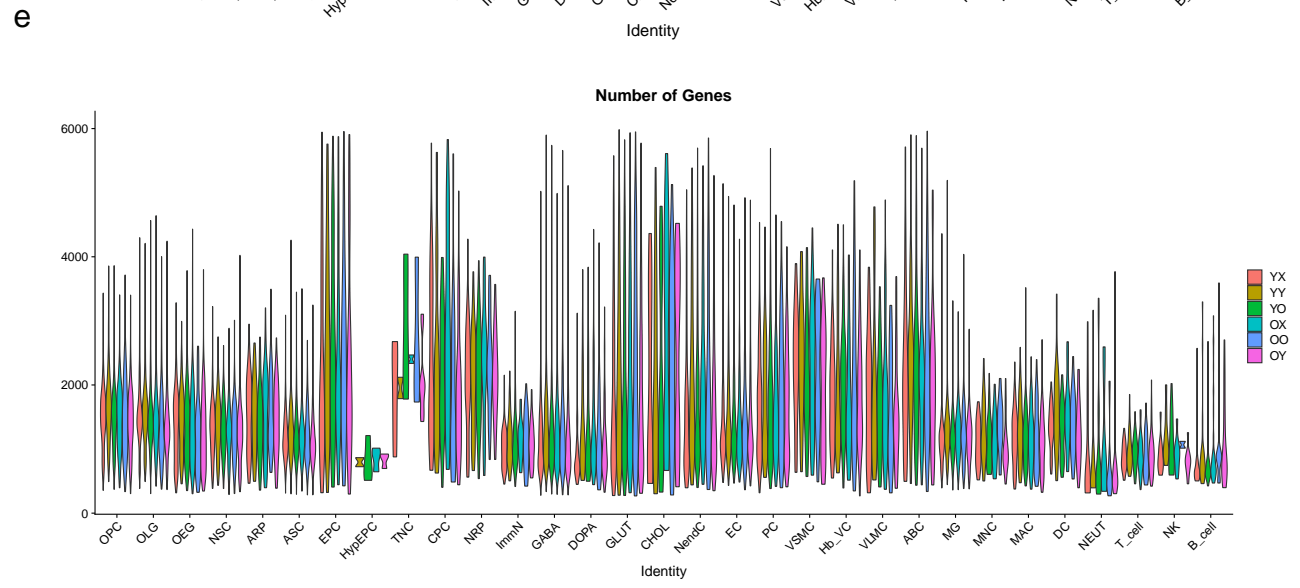
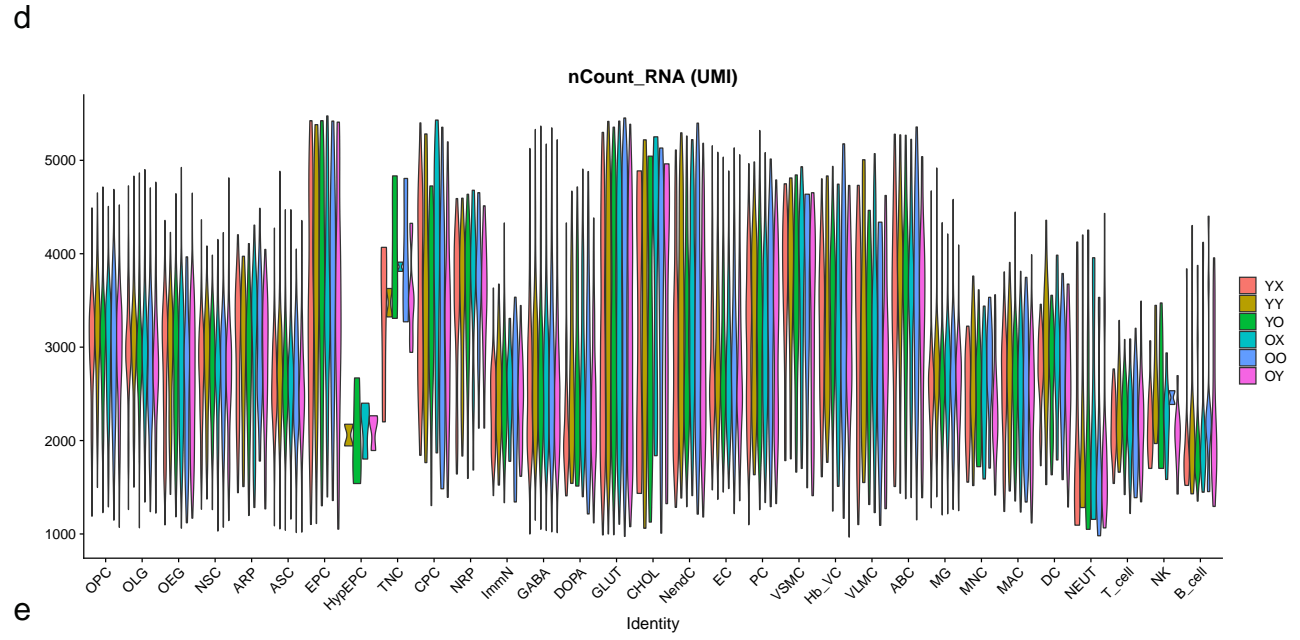
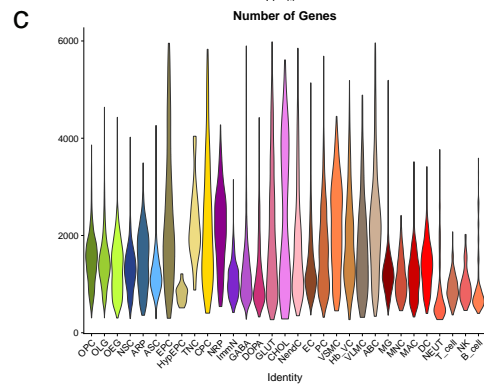
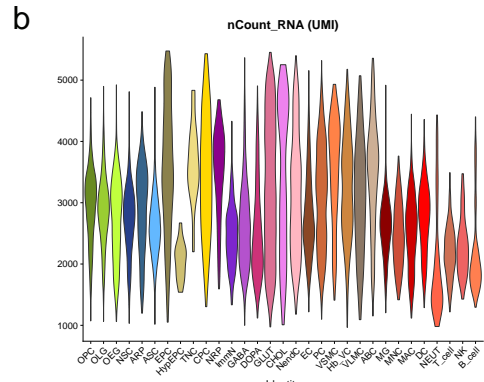
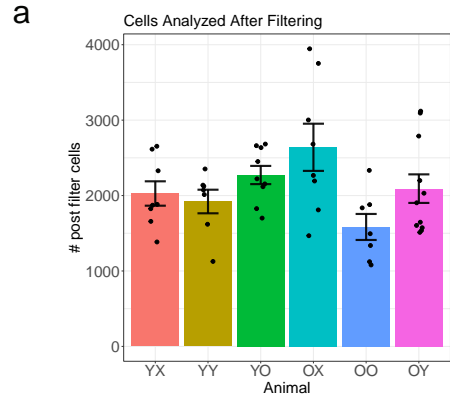


b



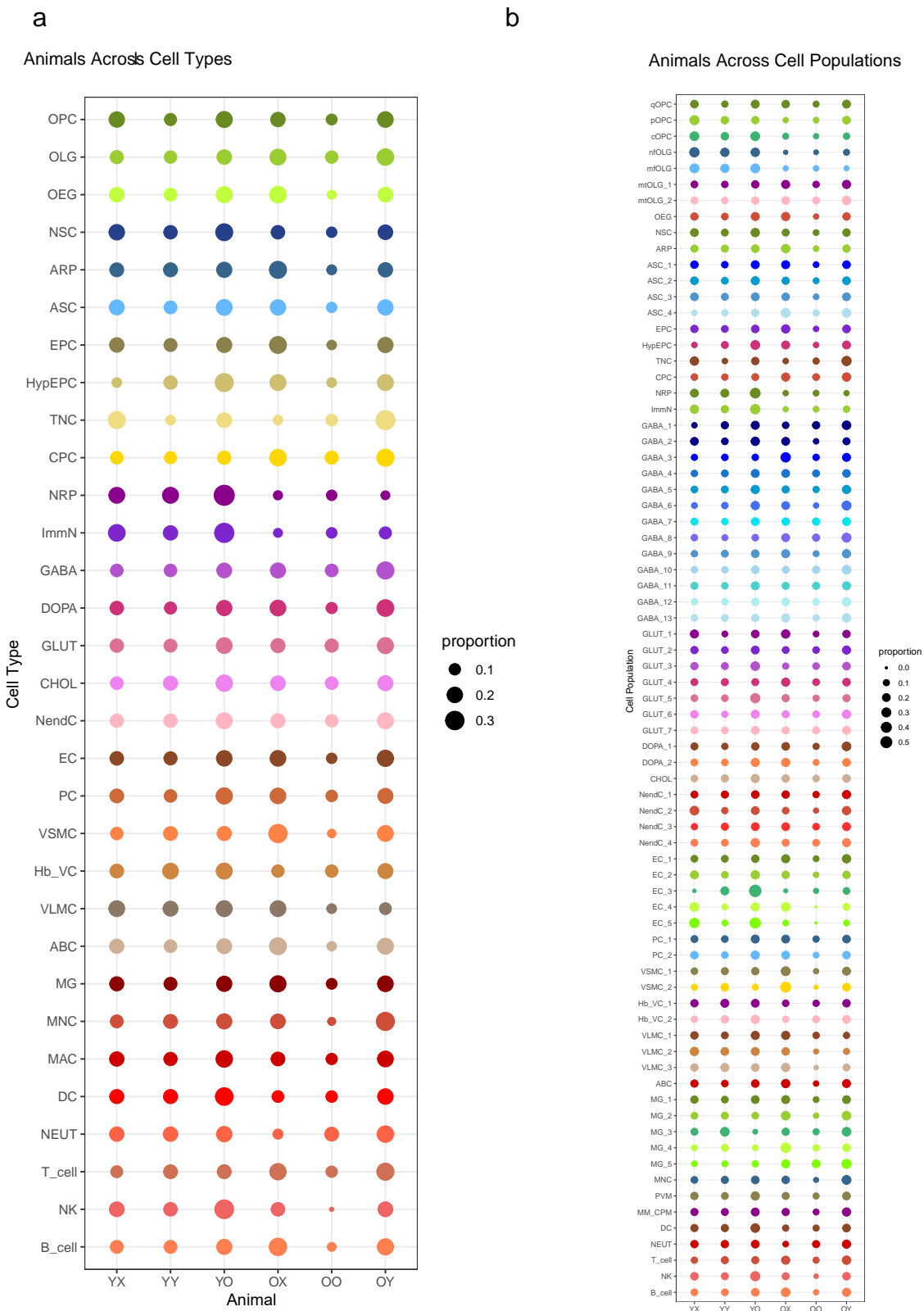
Supplementary Fig 4. Distribution of 50 animals across 5 sequencing batches, with respect to cell clusters. **a.** UMAP projection of color-coded batches over clusters that passed filtering criteria. **b.** Frequency of each color-coded batch representation in each cell type. All cell types are represented by cells from all batches, except for HypEPC in batch 5, probably due to its small size.

Fig_S5



Supplementary Fig 5. Primary data analysis. **a.** Bar plot showing the number of cells analyzed by animal after cell filtering, in which all cells were successfully assigned to a specific cell type (data presents mean \pm SEM). **b-e.** Violin plots showing QC metrics, plots in (b, c) showing aggregated data of cells of all brain types, while plots in (d, e) showing individual cell data separated by animal type: (b, d) showing nCount RNA (UMI) per cell type. (c, e) showing nFeature RNA (number of unique genes) detected per cell.

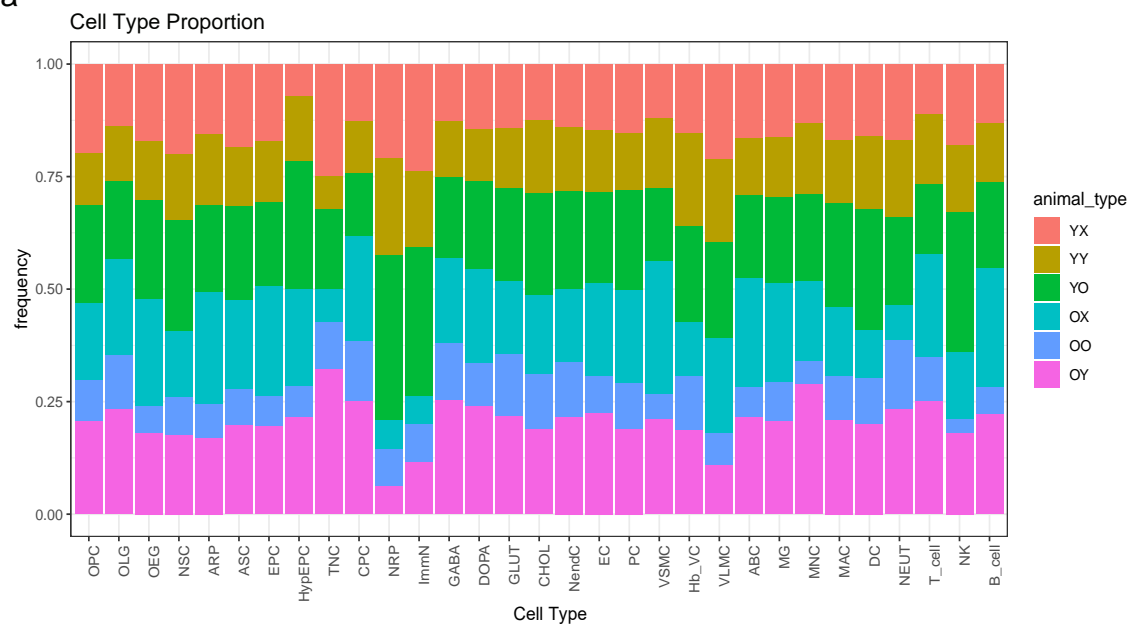
Fig_S6



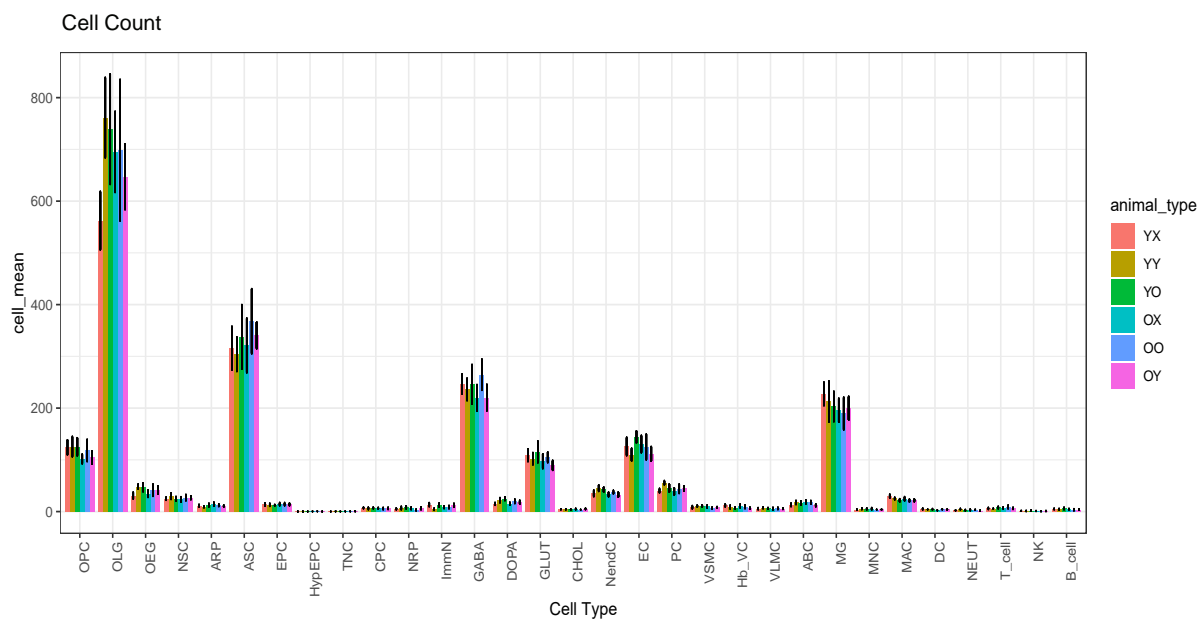
Supplementary Fig 6. Representation of each animal type's distribution within each cell type. **a.** Dot plot representation of each cell type's representation by each animal type. Size of the dot is proportional to the number of cells contributed by each animal type within a cell type. **b.** Dot plot representation of each subpopulation's representation by each animal type. Size of the dot is proportional to the number of cells contributed by each animal type within a subpopulation.

Fig_S7

a

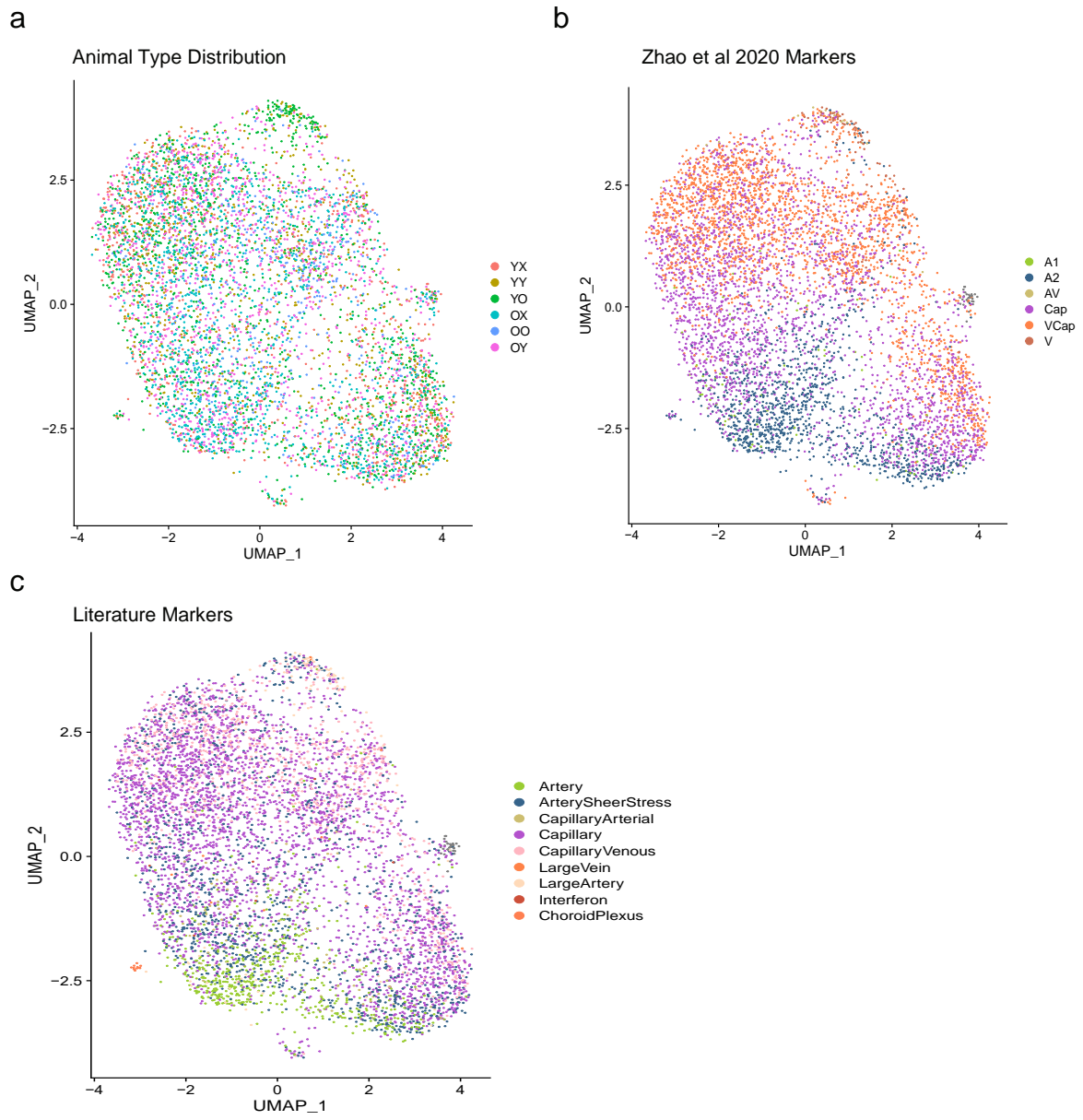


b



Supplementary Fig 7. Cell type composition and cell count from each animal type. a. Frequency bar plot demonstrating composition of each cell type with respect to animal type. **b.** Bar plot of raw cell counts, +/- SEM, with respect to each animal. All animals contribute to all cell types. ANOVA p-values for pairwise iterations can be found in Supplementary Table 2.

Fig_S8

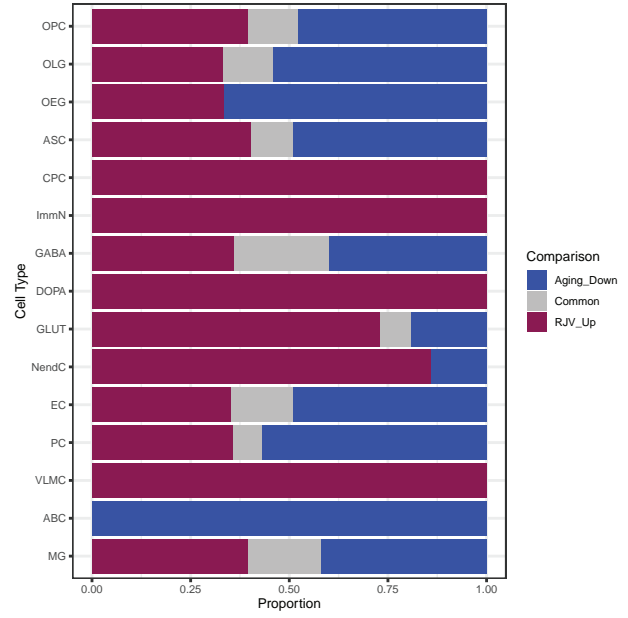
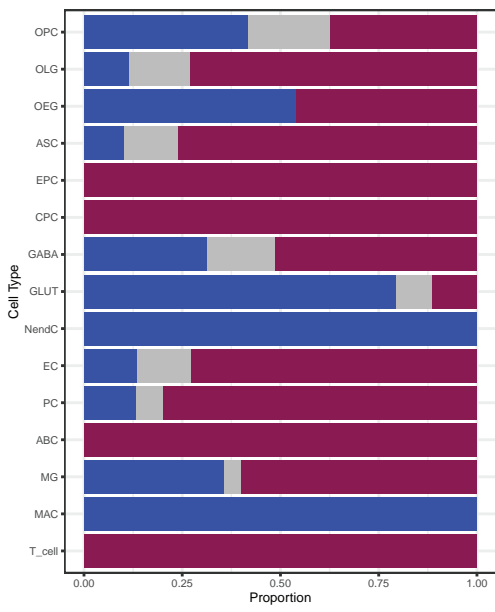


Supplementary Fig 8. Animal type distribution and machine learning approaches to explore EC arteriovenous zonation. **a.** Animal type cell distribution across EC subclusters. **b-c.** Probabilistic programming cell class assignment using EC marker genes described by Zhao et al 2020⁴ (b) and others^{4,3,2} (c).

Fig_S9

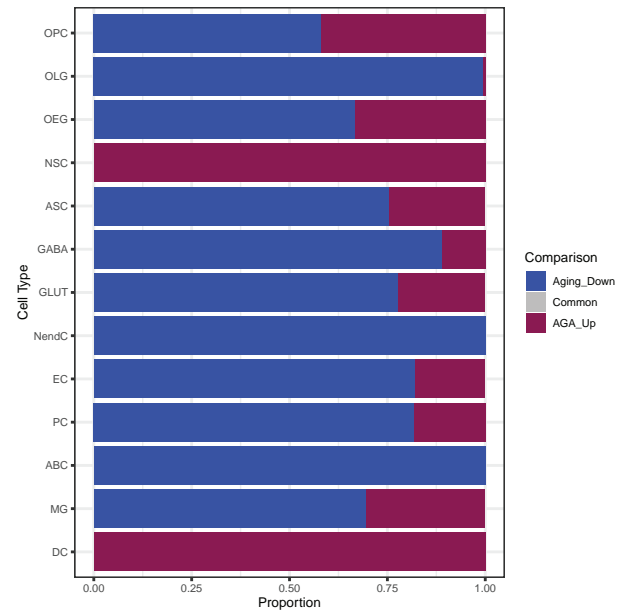
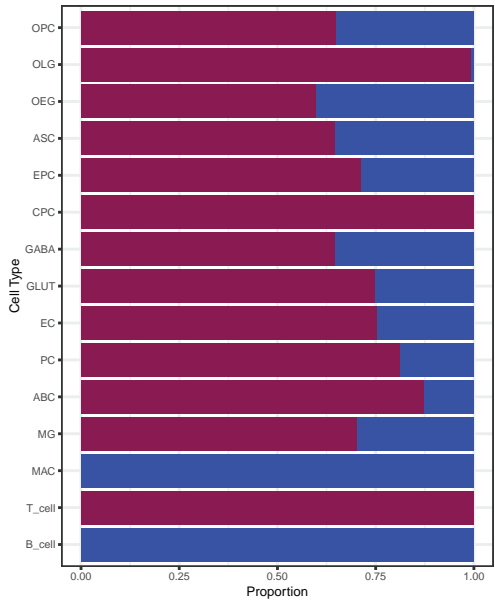
a

Aging-RJV



b

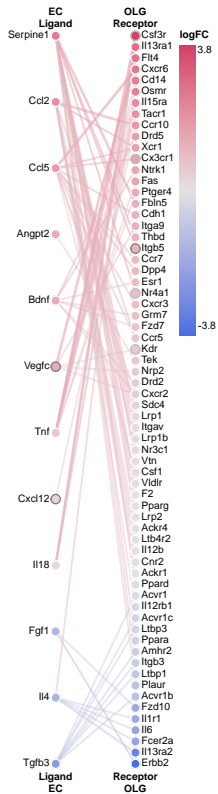
Aging-AGA



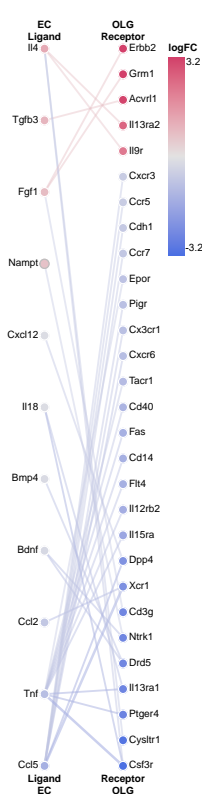
Supplementary Fig 9. Composition of DGEs per cell type between Aging-RJV, and Aging-AGA. **a.** Bar graph of each cell type's total $FDR \leq 0.05$ DGEs split by logFC direction. The proportion of DGEs reflecting Aging and RJV is depicted, as well as the fraction of overlapping signatures (intersection in grey). **b.** Bar graph of each cell type's total $FDR \leq 0.05$ DGEs split by logFC direction. The proportion of DGEs reflecting Aging and AGA is depicted, as well as the fraction of overlapping signatures (intersection in grey).

Fig_S10

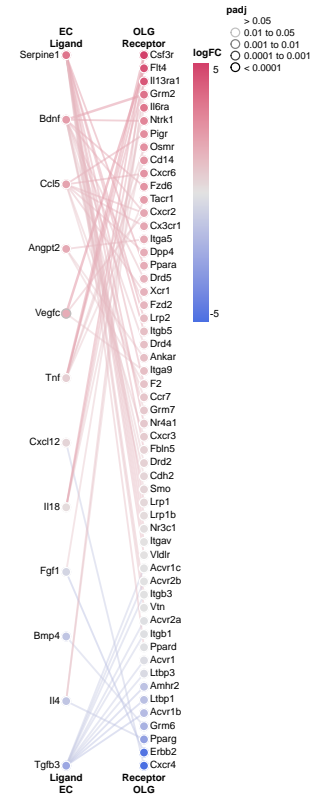
a
Aging



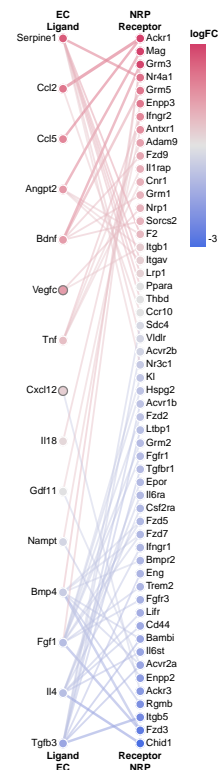
RJV



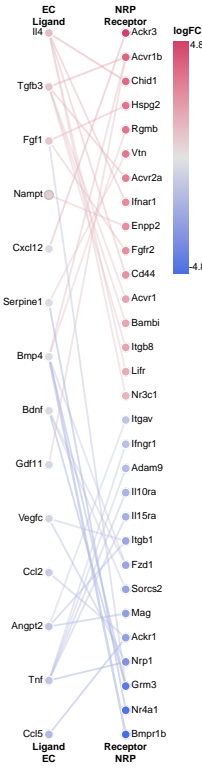
AGA



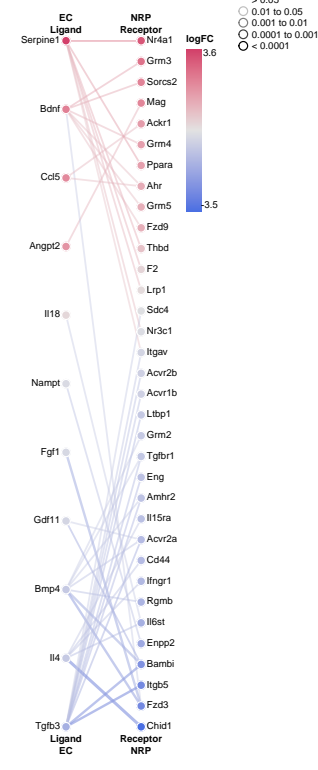
b
Aging



RJV



AGA



Supplementary Fig 10. Intercellular communication networks between EC-OLG and EC-NRP revealed aging-related interactions that were modified by heterochronic parabiosis. Canonical EC ligands and their cognate receptors in OLG (a) or in NRP (b) are shown in each paradigm (Aging, RJV, AGA). In all panels of ligand-receptor interactions, node color represents the magnitude of the DGE (logFC as estimated by DGE) such that the most significantly up-regulated genes are in magenta, and the downregulated genes are in blue. Node borders indicate FDR statistical significance of DGE. Edge color represents the sum of scaled differential expression magnitudes from each contributing node, while width and transparency are determined by the magnitude of the scaled differential expression (see details in the Methods section).

Supplementary Tables

Supplementary Table 1. List of abbreviations for all cell types and subpopulations.

Supplementary Table 2. Metrics of pairwise comparison of cell types by cell number. For each pairwise comparison, per cell type, ANOVA was applied, with significance designation (ns padj > 0.05, * padj ≤ 0.05, ** padj ≤ 0.01, *** padj ≤ 0.001).

Supplementary Tables 3-11. DGE metrics per comparison, per cell type. edgeR/muscat metrics were computed for each cluster in a comparison, with logFC, p-value, Benjamini-Hochberg p-value adjustment (p_adj.loc is per cluster, p_adj.global is with respect to all clusters in class) reported. TPM values (“tpm”) for each animal type, per cell type are listed. Percentage expression (“pct”) of each gene for each animal type, per cell type are listed.

RJV=Rejuvenation-association ((OY-OX)-(OO-YX)), AGA=Aging Acceleration-associated ((YO-YX)-(YY-OX)), Aging=OX/YX, OY_OO=OY/OO, OY_OX=OY/OX, OO_OX=OO/OX, YO_YY=YO/YY, YO_YX=YO/YX, YY_YX=YY/YX. HypEPC and TNC clusters did not have enough cells distributed across multiple animals for inclusion in the DGE framework, but TPM and PCT are reported.

Supplementary Table 12. RJV and Aging common DGEs and unique DGEs, per cell type. DGE FDR ≤ 0.05 genes common between RJV and Aging, but also those only found in RJV, and those only found in Aging are listed per cell type.

Supplementary Table 13. AGA and Aging common DGEs and unique DGEs, per cell type. DGE FDR ≤ 0.05 genes common between AGA and Aging, but also those only found in AGA, and those only found in Aging are listed per cell type.

Supplementary Table 14. DGE bi-directional DGEs between RJV and AGA. For RJV and AGA DGE genes FDR ≤ 0.05 per cell type, report the genes that are RJV Up (logFC >0) and AGA Down (logFC <0), or RJV Down (logFC <0) and AGA Up (logFC >0). Count is the number of times a gene is bi-directionally expressed across cell types.

Supplementary Table 15. Matrices of all DGE FDR ≤ 0.05 logFC values across cell types. Per comparison, per gene, clusters where the gene’s significance is FDR ≤ 0.05 have their logFC value reported. “Up” column is the sum of clusters with logFC >0, “Down” column is the sum of clusters with logFC < 0.

Supplementary Table 16. DGE logFC values across all cell types. Per comparison, per gene, collated logFC values across all clusters reporting DGE, with no thresholding. “Up” column is the sum of cell types with logFC >0, “Down” column is the sum of clusters with logFC < 0.

Supplementary Table 17. Matrices of all identified significant GSEA terms per comparison across cell types. fGSEA Benjamini-Hochberg adjusted p-value ≤ 0.25 significant terms are collated per comparison across all cell types by Normalized Enrichment Score (NES). Pathway and process metaclasses are described in the Methods. “Up” column is the sum of cell types with NES >0, “Down” column is the sum of cell types with NES < 0.

Supplementary Table 18. SCENIC regulon matrices per animal type. Per animal type, per cell type, SCENIC regulon activity scores are reported. Column “counts” is the sum of cell type that have a regulon score.

Supplementary Table 19. Cell-cell communication networks in RJV, AGA, and per animal type. For RJV, the set of unique source:target:receptor:ligand pairs that are found only in OY and YX combined. For AGA, the set of unique source:target:receptor:ligand pairs that are found only in YO and OX combined. YX, YY, YO, OX, OO, OY display the CellChat⁷ networks derived for each animal type (see details in Methods). “Source” is the cell type the ligand comes from,

while “Target” is the cell type found matching the ligand’s receptor. Probability and p-value are the statistical measures derived by CellChat. Ligand-Receptor pairs are given Interaction Names and assigned to a Pathway. Annotation provides the type of interaction are Secreted Signaling, ECM-Receptor, Cell-Cell Contact. Evidence codes and relevant PMIDs are provided by CellChat.

Supplementary Table 20: Literature-curated senescence-associated genes. Senescence-associated genes were curated from the literature for use as a reference gene set to perform fGSEA. HGNC.symbol denotes *Homo sapiens* gene symbol, MGI.ID denotes MGI ID number, MGI.symbol is *Mus musculus* gene symbol, Name is long name of the gene, and Feature Type denotes the type of gene or pseudogene.

Supplementary Table 21: Senescence status GSEA per comparison. For RJV, AGA, and aging, fGSEA against a literature-curated senescence gene set (Supplementary Table 20) to derive enrichment score, Normalized Enrichment Score (NES), p-value, Benjamini-Hochberg adjusted p-value, rank, and genes in the leading edge.

References

- 1 Ximerakis, M. *et al.* Single-cell transcriptomic profiling of the aging mouse brain. *Nat Neurosci* **22**, 1696-1708, doi:10.1038/s41593-019-0491-3 (2019).
- 2 Vanlandewijck, M. *et al.* A molecular atlas of cell types and zonation in the brain vasculature. *Nature* **554**, 475-480, doi:10.1038/nature25739 (2018).
- 3 Kalucka, J. *et al.* Single-Cell Transcriptome Atlas of Murine Endothelial Cells. *Cell* **180**, 764-779 e720, doi:10.1016/j.cell.2020.01.015 (2020).
- 4 Zhao, L. *et al.* Pharmacologically reversible zonation-dependent endothelial cell transcriptomic changes with neurodegenerative disease associations in the aged brain. *Nat Commun* **11**, 4413, doi:10.1038/s41467-020-18249-3 (2020).
- 5 Coppe, J. P., Desprez, P. Y., Krtolica, A. & Campisi, J. The senescence-associated secretory phenotype: the dark side of tumor suppression. *Annu Rev Pathol* **5**, 99-118, doi:10.1146/annurev-pathol-121808-102144 (2010).
- 6 Yousefzadeh, M. J. *et al.* Heterochronic parabiosis regulates the extent of cellular senescence in multiple tissues. *Geroscience* **42**, 951-961, doi:10.1007/s11357-020-00185-1 (2020).
- 7 Jin, S. *et al.* Inference and analysis of cell-cell communication using CellChat. *Nat Commun* **12**, 1088, doi:10.1038/s41467-021-21246-9 (2021).